Soil Transport by Winds on Mars

BRUCE R. WHITE

University of California, Davis, California 95616

The eolian transport of surface material on the planet Mars is estimated from results of low-pressure wind tunnel testing and theoretical considerations. A semiempirical relation is developed that will estimate the total amount of surface material moving in eolian saltation, suspension, and surface traction. The estimated total mass movement of surface material per unit width time on the surface of Mars is $q = 2.61\rho(V_* - V_{*t})(V_* + V_{*t})^2/g$ (g/cm s), where ρ is the density of the atmospheric gas, g is the acceleration due to gravity, and V_* and V_{*t} are the friction speed and saltation threshold friction speed, respectively. A flat surface composed of particles of nearly uniform size is assumed. A change in the mean particle size changes the threshold friction speed V_{*t}. The path lengths of saltating particles and wavelengths of surface ripples can vary as much as a factor of 2 if the surface temperature varies from 150 to 250 K. The angles between particle paths and the horizontal surface are calculated to be lower on Mars than on earth, and particles travel much faster on Mars than on earth. The ratio of final particle velocity to threshold friction speed, V_F/V_{*t}, is found to be several times that of saltation on earth.

INTRODUCTION

This paper presents three aspects of the movement of surface material by wind on Mars and assembles them to estimate transport rates. First, the governing equations of motion are presented and their numerical solutions. These are discussed with applications to Mars. Second, an analytical theory is presented from which one may estimate the surface flux. Last, results from low-pressure wind tunnel experiments are presented and are used to complete the semiempirical relationship. The last two sections are in good agreement with basic characteristics of particle motion as determined by the numerical solutions. The numerical results pertain directly to Mars, while the experimental work is performed at reduced pressure to simulate Martian conditions. The resulting transport equation is, however, applicable to both earth and Mars.

SALTATION ON MARS

The movement of material by windblown (eolian) processes can be by surface traction, saltation, and suspension. Surface traction is the movement along the surface. Saltation refers to a leaping motion of particles where they lift off the surface and travel in ballistic type trajectories returning to the surface. In the case of suspension the particles leave the surface in the same manner as that of saltation; however, they do not return directly to the surface. The vertical turbulent velocity fluctuations are large enough (greater than the terminal falling speeds) to keep the particles suspended. For every size particle there is a minimum wind speed necessary to create motion. Associated with the wind speed is the surface shear stress τ that is a result of the gas motion above the surface. The velocity diminishes to zero at the surface for the case of continuum flow (e.g., where the Knudsen number, the ratio of the mean free path length between molecular collisions of molecules to a characteristic length of the flow, is very small). For all terrestrial flows containing saltating material the continuum assumption is valid, but it is not always valid on Mars. As the gas pressure and density are reduced in the Martian atmosphere, the Knudsen number begins to increase. At a value of 0.1 or so, noncontinuum effects of the flow must be considered in the analysis.

Bagnold [1941] had demonstrated that at the initiation of saltation,

$$\tau_t = A^2(\rho_p - \rho)gD_p \tag{1}$$

where τ_t is the surface shear stress at threshold, A is a varying empirical coefficient, ρ_p is the particle density, ρ is the fluid density, g is the acceleration due to gravity, and D_p is the mean particle diameter. This expression is commonly rewritten in terms of the friction speed at threshold $V_{*t}^2 = \tau/\rho$ as

$$V_{*t} = A\{[(\rho - \rho_p)/\rho]gD_p\}^{1/2} \tag{2}$$

When the particle density is much greater than the fluid density, this expression reduces to

$$V_{*t} = A(\rho_p gD_p/\rho)^{1/2} \tag{3}$$

Bagnold as well as other investigators demonstrated that A is only a function of the particle friction Reynolds number, $B = V_{*t}D_p/\nu$, for the threshold condition. Here ν is the kinematic viscosity of the fluid. This condition of $A = A(B)$ is true only only of terrestrial saltation. Figure 1 shows the A versus B curve displaying terrestrial wind tunnel data. Here the particle diameters range from a few microns to approximately 1.4 mm, and the particle density varies from 0.2 g/cm to 11.4 g/cm. This gives a fairly wide range of conditions to demonstrate the terrestrial uniqueness of the curve. Recently, low-pressure wind tunnel tests [*Greeley et al.*, 1977] have demonstrated that $A = A(B)$ is not unique for atmospheric pressures different from the earth's. Other forces, previously not considered, seem to have a strong functional dependence on the ambient pressure. Such forces include electrostatic and interparticle reactions; these seem to alter the empirical coefficient A in a manner not fully understood. Figure 2 shows a plot of a dimensionless friction speed, $(A^2B)^{1/3}$ versus a dimensionless diameter $(B/A)^{2/3}$. These data were taken from experimental work using a low-pressure wind tunnel located at NASA Ames Research Center, Moffett Field, California. The test material was ground walnut shell that was sieved to the shown particle size distribution on the figure. If A is only a function of B regardless of pressure. all data should be fitted by one universal curve. However, as shown on the graph, this is not the case, and the data seem to depend strongly on particle diameter; each particular particle diameter yields its own curve on the plot.

EQUATIONS OF PARTICLE MOTION

A one-dimensional flow situation is assumed to calculate the trajectories in which the velocity in the vertical (y) direction is

Paper number 9B0222.
0148-0227/79/009B-0222$01.00

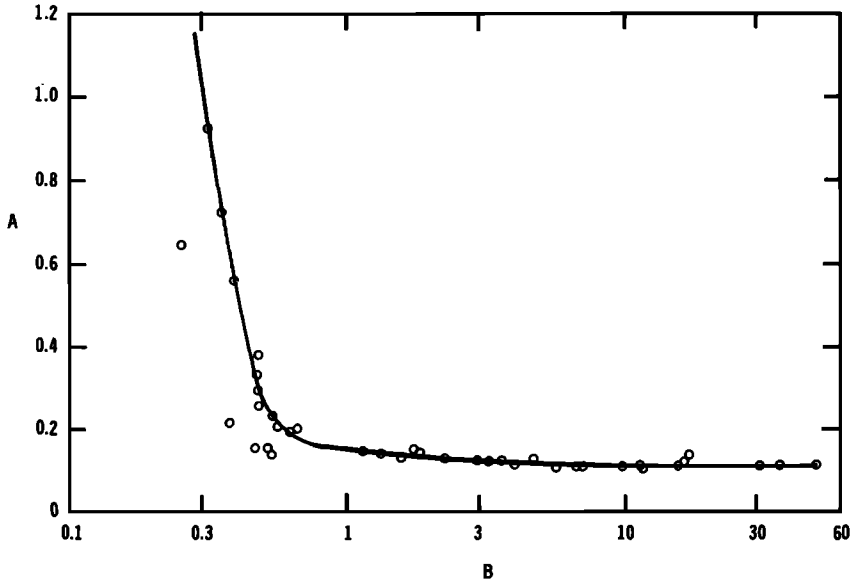

Fig. 1. Bagnold's coefficient A as a function of the threshold particle friction Reynolds number $B = V_{*t} D_p/\nu$. This is a unique curve for atmospheric pressure. A obtains a constant value of 0.118 for values of B greater than 10.

zero and the velocity u in the flow (x) direction is a function of height above the surface only. A viscous sublayer exists for flow over a surface of like particles on Mars when the wind speed is below threshold [*White et al.*, 1976]. However, when minimum threshold speeds are reached, the optimum size particles begin to saltate. This consequently breaks up the viscous sublayer, and a fully turbulent boundary layer is formed. The presence of saltating particles significantly alters the nature of the velocity profiles as described by *White and Schulz* [1977] and is represented by

$$\frac{u}{V_*} = 2.5 \ln (y/D_p) - 2.29 + 1.79 \frac{V_{*t}}{V_*} \tag{4}$$

where u is the velocity in the flow direction, V_* is the friction speed, and D_p is the average particle diameter. As V_* approaches V_{*t}, this equation approaches the velocity profile of the fully developed nonsaltating turbulent boundary layer.

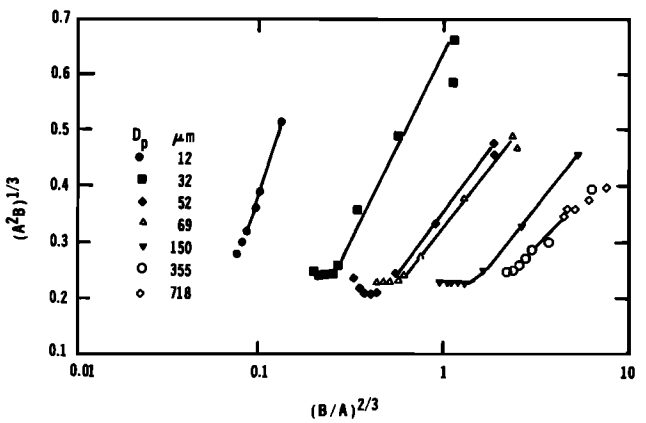

Fig. 2. Dimensionless threshold friction speed $(A^2B)^{1/3}$ as a function of dimensionless particle diameter $(B/A)^{2/3}$ for several different particle distributions all having an equal particle density of 1.1 g/cm³. The pressure ranged from a minimum of 5 mbar (0.5 kPa) to 1 atm. If Bagnold's coefficient A is uniquely only a function of B for the range of pressures tested, then only a single curve should suffice to fit all the experimental data. This is not the case, since each separate particle diameter range exhibits its own curve. Hence $A = A(B)$ only is not the case when the atmospheric pressure is varied or altered.

The forces acting on a saltating particle are a downward force due to gravity, the aerodynamic drag force D acting opposite the direction of relative particle velocity V_r, and the lift force L acting normal to the drag force. The equations for translational motion of a particle can be written as

$$m_p \ddot{x} = L \frac{\dot{y}}{V_r} - D \frac{\dot{x} - u}{V_r} \tag{5}$$

$$m_p \ddot{y} = -L \frac{\dot{x} - u}{V_r} - D \frac{\dot{y}}{V_r} - m_p g \tag{6}$$

where m_p is the particle's mass, $(\dot{x}, \dot{y})$ and $(\ddot{x}, \ddot{y})$ are the particle's velocity and acceleration components, and g is the acceleration due to gravity.

In (5) and (6),

$$V_r = [(\dot{x} - u)^2 + \dot{y}]^{1/2} \tag{7}$$

The effects of lift and drag are expressed in terms of lift and drag coefficients C_L and C_D, defined by

$$L = \tfrac{1}{8} C_L \pi \rho D_p^2 V_r^2 \qquad D = \tfrac{1}{8} C_D \pi \rho D_p^2 V_r^2 \tag{8}$$

Assuming the particles are spherical and of uniform density, the equations of motion reduce to

$$\ddot{x} = -\frac{3}{4} \frac{\rho}{\rho_p} \frac{V_r}{D_p} [C_D (\dot{x} - u) - C_L \dot{y}] \tag{9}$$

$$\ddot{y} = -\frac{3}{4} \frac{\rho}{\rho_p} \frac{V_r}{D_p} [C_D \dot{y} + C_L (\dot{x} - u)] - g \tag{10}$$

where ρ_p is the particle density.

The drag coefficient of a sphere is strongly dependent upon the Reynolds number. The empirical formulas of *Morsi and Alexander* [1972] are used for its determination in the numerical calculations. The initial conditions are same as those used by *White et al.* [1976]. Initially, the particle is at rest on the surface, and as the wind speed is increased above threshold, particles begin to move. The expressions for the lift coefficients are presented by *White et al.* [1976]. The reader may wish to review an in-depth discussion of this numerical solution procedure, including a complete discussion of this technique, in the work of *White et al.* [1976].

TABLE 1. Values of Gas Density, Viscosity, Mean Free Path, and Particle Fall Speed for Various Surface Pressures and Temperatures

	Surface Pressure, kPa					
	0.25		0.75		1.5	
	150 K	250 K	150 K	250 K	150 K	250 K
Gas density ρ, $\times 10^5$ g/cm^3	0.882	0.529	2.65	1.59	5.29	3.18
Kinematic viscosity ν, cm^2/s	8.59	23.8	2.86	7.94	1.43	3.97
Mean free path λ,* μm	9.59	20.6	3.20	6.87	1.60	3.43
Particle fall speed,† cm/s						
0.5 μm	1.11×10^{-1}	1.44×10^{-1}	3.64×10^{-2}	4.75×10^{-2}	1.82×10^{-2}	2.35×10^{-2}
1.0 μm	2.20×10^{-1}	2.86×10^{-1}	7.27×10^{-2}	9.42×10^{-2}	3.76×10^{-2}	4.69×10^{-2}
2.0 μm	4.36×10^{-1}	5.68×10^{-1}	1.50×10^{-1}	1.88×10^{-1}	8.59×10^{-2}	9.65×10^{-2}
10.0 μm	2.46	2.85	1.27	1.16	9.87×10^{-1}	7.88×10^{1}
50.0 μm	26.1	21.6	20.4	14.2	19.0	12.4

*The mean free paths are calculated by Maxwell's technique, as described by *Bird et al.* [1960, p. 21]; here $3\mu = \rho\bar{u}\lambda$, where $\bar{u}$ is the molecular velocity relative to the fluid velocity and μ is the absolute viscosity.

†The particle fall speeds include the effects of slip flow around the particle. The correction factor of *Davies* [1945] is used in the determination of the drag coefficient.

For calculations in the Martian atmosphere it is necessary to include the effects of slip flow caused by the rarefied atmosphere. The correction factor of *Davies* [1945] is used to calculate the slip flow effects. The mean free path needed in the Davies equation is calculated by a conventional Chapman-Enskog technique (see Table 1). The slip flow factor only becomes significant for the smaller-sized particles in the calculations. Figure 3 displays a typical particle trajectory and identifies the important parameters.

COMPUTATIONAL RESULTS

This section examines the dependence of the particles' trajectory path lengths as functions of several key parameters presented in Table 2, which summarizes the nominal and alternative parameter values used in the calculations. One parameter is allowed to vary at a time. A broad range of surface pressures and temperatures is explored. The nominal case is an approximate average of the surface data received from Viking Lander 1 site. The atmospheric gas composition used in the nominal calculation is equal to 100% carbon dioxide. A sensitivity study shows this to be valid within a few percent of the actual atmospheric gas composition.

Atmospheric surface pressures P vary greatly with time and location on Mars. At the bottom of the larger basins such as Hellas Planitia the pressure may be as high as 10–15 mbar (1–1.5 kPa) with some seasonal variation. The surface pressure is only a few millibars atop the large shield volcanoes. *Kliore et al.* [1972, 1973] have estimated an average pressure for Mars of about 6 mbar. Data from Viking indicate that the mean pressure may shift upward slightly. There will be substantial changes in gas density ρ and gas temperature T with such dramatic changes in pressure. The large changes in gas temperature and density may greatly alter the prevailing shearing rates associated with the winds and thus greatly alter the saltation characteristics of eolian movement.

Figure 4 shows the estimated threshold wind speeds necessary to initiate particle motion for various surface pressures for a range of particles from a diameter of 10 μm to 1 mm. Also shown is the speed of sound, above which the wind speed would not likely be reached in a planetary atmosphere. Such wind speeds are improbable, since the large amounts of turbulence associated with them would not allow transonic or supersonic flow [*Pollack et al.*, 1976*a*].

Figure 5*a* shows the dependence of the 'typical' path length of saltating particles on the particle diameter D_p for values of friction speed V_* ranging from 5 to 10 m/s. The numerically simulated surface conditions correspond to the values obtained by the Viking Lander 1, with a mean surface pressure of 7.5 mbar (0.75 kPa) and a minimum gas temperature of 187.2 K. The average heights that saltating particles obtained are 4–5 m above the surface for a friction speed of 10 m/s. This value of V_* would be encountered rarely on Mars, considering general circulation theories [*Pollack et al.*, 1976*b*]. It should act as an estimate in obtaining an upper limit value of the saltating grains. A more realistic case is that of V_* equal to 2.5 and 5 m/s. The first case, near threshold conditions (not displayed on the figure), shows only minute leaps. These saltating particles have relatively high collision impact angles α, with many of the larger particles not moving. These may be of primary importance in the final ripple pattern geometry when either a major sand storm subsides or when wind just surpasses threshold but fails to continue to grow in strength. The friction speed of 5 m/s shows saltation average maximum heights from 0.4 to 1 m. These heights of saltating grains are comparable to those found on earth. The path lengths are from 3 to 10 m. The particles smaller than 10 μm would, if injected into the wind by

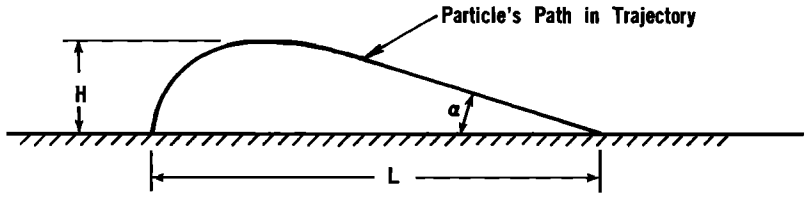

Fig. 3. A typical path of particle's trajectory. H is the maximum height the particle obtains in the trajectory, while L is the maximum jump length or path length obtained; α is the collision angle which the particle's path makes with the surface upon impact.

TABLE 2. Values of the Parameters Used in the Calculations of Particle Trajectories and Ripple Wavelengths

Parameter	Symbol	Nominal Value	Alternative Value
Surface pressure	P	7.5 mbar (0.75 kPa)	2.5, 5, 10, 15 mbar (0.25, 0.5, 1.0, 1.5 kPa)
Gas temperature near the ground*	T	187, 242 K	150, 250 K
Acceleration of gravity	g	372 cm/s^2	...
Von Kármán constant	k	0.4	...
Roughness height	y_0	$D_p/30$	immovable roughness elements
Dynamic viscosity†	μ	...	adjusted to the value appropriate for T
Molecular weight	...	44.01	43.65
Atmospheric composition	...	100% CO_2	96.1% CO_2, 2.2% N, 1.5% Ar, 0.1% O_2, 0.1% CO
Particle density	ρ_p	2.58 g/cm^3	1.55, 3.54 g/cm^3
Particle diameter	D_p	10^1–10^4	...
Friction speed‡	V_*	2.5, 5.0, 7.5, 10.1 m/s	can account for varying atmospheric stabilities

*These gas temperature values represent the minimum and maximum temperatures experienced by the Viking Lander 1 spacecraft during the first 20 sols as reported by *Hess et al.* [1976]. These are not intended to represent the absolute variation at the Viking Lander 1 site but rather provide a reasonable estimate of a minimum and maximum value of temperature.

†The values of μ were obtained from the procedure described by *Bird et al.* [1960, pp. 19–26]. The kinematic viscosity ν equals μ/ρ. Note that in contrast to ν, μ depends only on gas temperature and composition.

‡The friction speed can account for changes in the atmospheric stability. Once the saltation is initiated, the prevailing profiles within the saltation layer appear to be independent of the atmospheric stability (see (4)). Hence all that is necessary to account for the atmospheric stability is to know the proper ratio of V_*/V_0, where V_0 represents some characteristic velocity at a particular height. Such information can be obtained from a recent paper by *Pollack et al.* [1976*a*], which presents friction velocity ratios for a variety of stability conditions.

impacting collisions, likely go into suspension, since their terminal falling speeds are small (see Table 1). This is shown by the long path lengths of smaller-particle trajectories.

Impact angles of particles colliding with the surface have a wide variation in values. The collision angle α decreases in value with increasing surface shear. A 0.15-mm particle has an impact angle of approximately 7°–10° near threshold (Figure 5*b*); and if the friction speed is increased to 5 m/s, the collision angle decreases to 3.6°. In comparison to earth these angles are unusually small for similar ratios of surface to threshold stress. The typical range of angles for particles greater than 0.4 mm is from 5° to 15°, which agrees with saltation on earth. The larger particles seldom saltate more than 6 to 10 m in path lengths.

Figure 6 shows results for a case like that of Figure 5*a* except

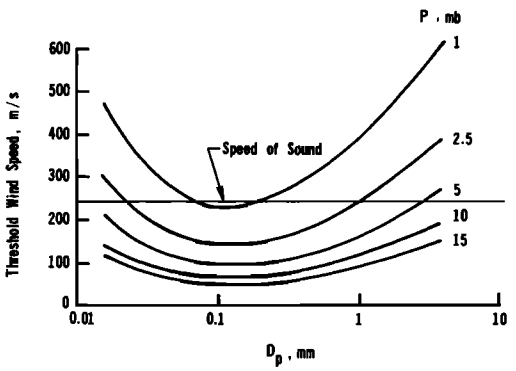

Fig. 4. Threshold wind speed for Mars as a function of particle diameter D_p for several values of the surface pressure p. The horizontal line represents the speed of sound at a temperature of 239 K [after *Pollack et al.*, 1976*a*].

the temperature is 241 K, the maximum measured by the Viking Lander 1 during the first sols (a sol is a Martian day). A drop in temperature from 241.8 to 187.2 K reduces the dynamic viscosity of the atmospheric gas on Mars by 22.7%. At a constant pressure of 0.75 kPa the gas density decreases 22.6%, drastically affecting the shear stress on the surface. The Reynolds number, ratio of inertia to viscous forces, is altered substantially. The change in flow around individual particles and the surface alters the pressure distribution around the particles. Hence this changes the typical path lengths of the saltating particles.

As the temperature is increased, the maximum heights and lengths of trajectories are generally curtailed. For the majority of the cases the characteristic path length is substantially shorter at the higher temperature. The maximum heights occurring in saltation on Mars have only minor deviation with change in temperature. Correspondingly, there are only small differences occurring in impact angles.

The trends exhibited in the path length, maximum height, and impact angle for a pressure of 7.5 mbar (0.75 kPa) are also present for other surface pressures. As an example, an extremely low pressure that may exist on the surface would be 2.5 mbar (0.25 kPa); Figures 7*a* and 7*b* demonstrate that the relationship between path length and height is a function of temperature. In these figures a low temperature of 150 K and a maximum of 250 K are used. The path lengths are curtailed as much as 50% with an increase in surface temperature of 100 K.

An examination of the final velocities the particles obtain shows increased values at the low temperatures. The final particle speeds are typically greater than V_*. The value depends on the boundary layer flow and V_*/V_g. (V_g is the wind speed near the top of the atmospheric boundary layer on Mars as described by *Pollack et al.* [1976*a*].) The value of V_g would

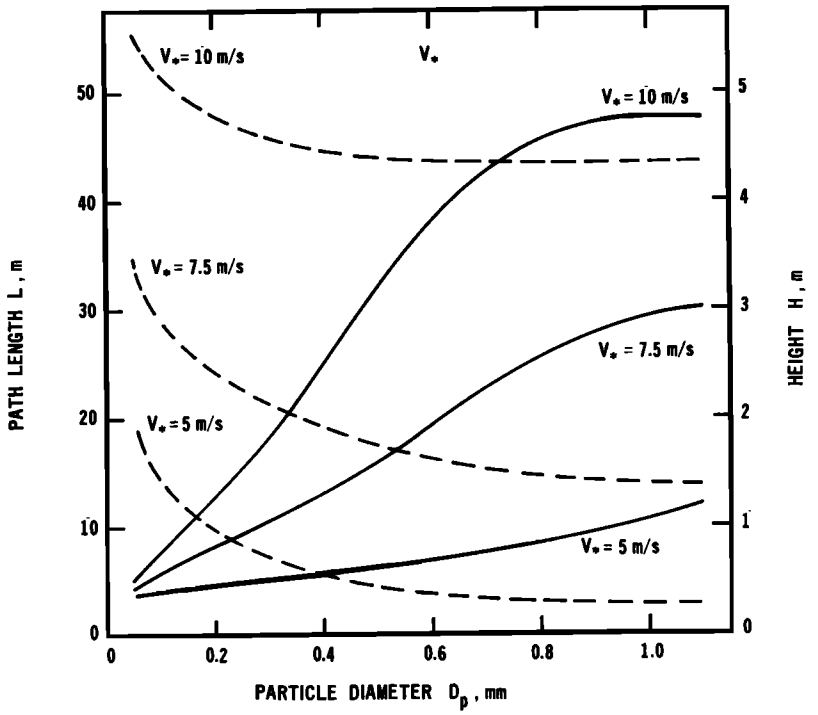

Fig. 5*a*. Typical path lengths L (dashed lines) and maximum vertical heights H (solid lines) for saltating particles as functions of particle diameter D_p for several values of surface friction speed V_*. The surface conditions correspond to a pressure of 7.5 mbar (0.75 kPa), a particle density of 2.58 g/cm^3, and a gas temperature of 187.2 K. Note the different scales for L and H.

be the maximum limit that the final speed of particles could obtain.

As the particle diameter decreases, it becomes more susceptible to turbulent velocity fluctuations in the boundary layer flow. When the terminal falling speed of the particles is less than the vertical component of turbulent fluctuations, the particles are in suspension. The turbulent eddies of the flow carry these particles aloft to high altitudes and are capable of transporting these particles long distances before they slowly and gradually return to the surface. This is in contrast to saltation, where the height and length of particles are only a few meters in value; however, particles in suspension may be carried up to altitudes of several kilometers and carried downstream distances of several thousand kilometers. A terrestrial

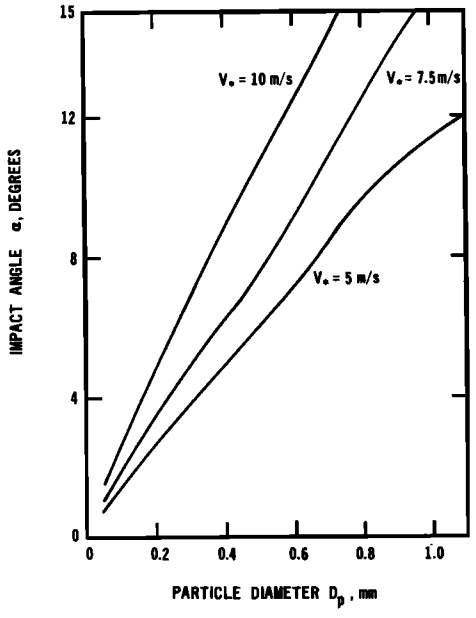

Fig. 5*b*. Impact angles α as a function of particle diameter D_p for several values of surface friction speed V_*. The surface conditions correspond to a pressure of 7.5 mbar (0.75 kPa), a particle density of 2.58 g/cm^3, and a gas temperature of 187.2 K.

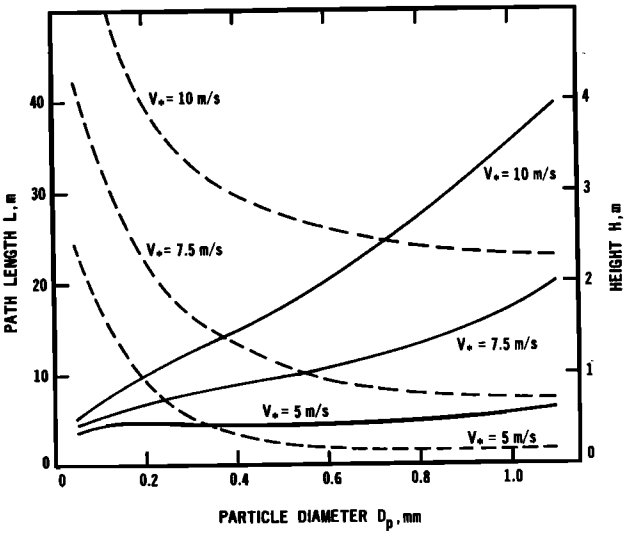

Fig. 6. Typical path lengths L (dashed lines) and maximum vertical heights H (solid lines) for saltating particles as functions of particle diameter D_p for several values of surface friction speed V_*. The surface conditions correspond to a pressure of 7.5 mbar (0.75 kPa), a particle density of 2.58 g/cm^3, and a gas temperature of 241.8 K. Note the different scales for L and H.

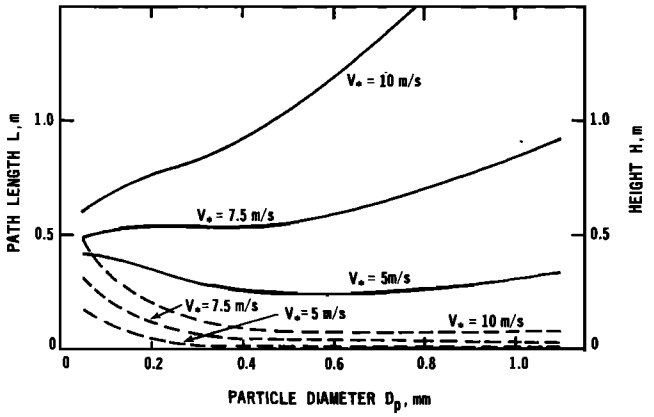

Fig. 7a. Typical path lengths L (dashed lines) and maximum vertical heights H (solid lines) as functions of particle diameter D_p for several values of surface friction speed V_*. The surface conditions correpsond to a pressure of 2.5 mbar (0.25 kPa), a particle density of 2.58 g/cm³, and a gas temperature of 150 K.

example of this is reported by *Yaalon and Ganor* [1977], in which Sahara dust (a few microns or less in diameter) was carried to the far eastern part of Asia, some 5000 km.

An analysis of the infrared interferometer spectrometer experiment on board Mariner 9 sized the majority of suspended particles from 0.1 to 10 μm in diameter in the Martian atmosphere. The boundary between suspendable and saltating particles is determined by a constant ratio of V_F/V_*, where V_F is the final particle speed in its trajectory [*Pollack et al.*, 1976*a*]. *Toon et al.* [1976] show that the Martian planetary boundary layer can support particles with fall speeds as large as 1 cm/s (10-μm-diameter particles at 0.75 kPa). The calculated ratio V_F/V_* is several times unity for these conditions. This is at variance with *Sagan and Bagnold* [1975], who suggest a ratio of unity. It seems reasonable that the ratio V_{F_M}/V_{F_E} will be larger

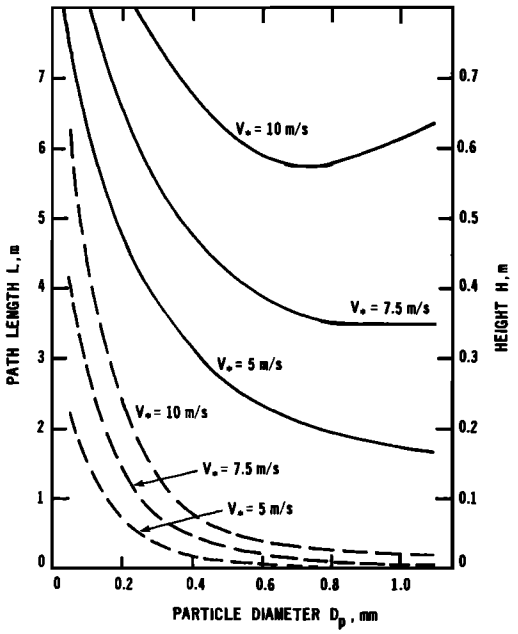

Fig. 7b. Typical path lengths L (dashed lines) and maximum vertical heights H (solid lines) as functions of particle diameter D_p for several values of surface friction speed V_*. The surface conditions correspond to a pressure of 2.5 mbar (0.25 kPa), a particle density of 2.58 g/cm³, and a gas temperature of 250 K. Note the different scales for L and H.

than unity on Mars for equal ratios of V_*/V_{*t}, where subscripts M and E indicate Mars and earth, respectively. From $V_*^2 = \tau/\rho$ and wind tunnel tests at low pressures [*Greeley et al.*, 1977] the threshold stress is about equal to that of the atmospheric case. Thus $\rho_E V_{*}^2/\rho_M V_{*M}^2$ is approximately equal to unity. Hence V_* is roughly 7 times greater; and comparing the ratios of V_g/V_* indicates that V_F on Mars is substantially larger than V_F on earth. These are also indicated in the numerical results; the ratio V_F/V_* is generally greater than unity for typical saltation and can go as high as 10, the latter definitely indicating particles going into suspension in numerical calculations.

In comparison with the nominal test case of 0.75 kPa the reduction in surface pressure to 0.25 kPa results in these differences: (1) the saltating particles are roughly decreased in height and path length by a factor of 2–4, (2) similarly, the ratio of maximum impact speed to V_* is reduced with decreases in pressure, and (3) the overall trajectory and scale of flux movement are reduced.

Analytical Determination of Surface Material Movement

The rate of movement of surface material under specified storm conditions is of primary interest for Mars. An estimate of the total amount of surface material transported by the wind may be made by examining the physics of the process. This will account for the changes in the Reynolds number and interparticle forces that occur with reduction of pressure. In order to estimate the surface flux the typical path lengths of saltation must be known, as described in the previous section.

The key parameter in estimating surface material movement rates is the characteristic path length of saltating particles. Several investigators have developed both empirical and theoretical methods to calculate path lengths [*Tsuchiya*, 1969; *Kawamura*, 1951; *Bagnold*, 1941]. Tsuchiya has a theoretical development on the successive saltating leaps. However, it is necessary to know the initial or maximum vertical component of velocity at lift-off for the particle in order to calculate its path length. This component is generally a function of the flow conditions. Formulation of this type, with the vertical velocity component a function of the path length, does not lend itself well to calculations of surface material movement. A more favorable expression is one where the path length depends on the ratio of surface to threshold stress. One such analysis is a force balance on a control volume [*Kawamura*, 1951]. The surface shear stress τ_0 consists of two elements. The first is the ordinary wind shear τ_{wind} developed from the motion of the gas flow over the surface. The second stress, τ_{sand}, stems from the impact of particles colliding with the surface:

$$\tau_0 = \tau_{\text{sand}} + \tau_{\text{wind}} \tag{11}$$

or

$$\tau_{\text{sand}} = \rho(V_* + V_{*t})(V_* - V_{*t}) \tag{12}$$

τ_{sand} is also equal to the momentum loss in the flow direction,

$$\tau_{\text{sand}} = M(V_f - V_i) \tag{13}$$

where M is the mass of material falling per unit area time, V_f is the mean final horizontal velocity component of the particles at collision with the surface, and V_i is the horizontal component of velocity during the initial lift-off of the particles from the surface. Assuming an inelastic collision

$$wM \sim \rho(V_*^2 - V_{*t}^2) \tag{14}$$

from experience,

$$M \sim \rho(V_* - V_{*t}) \tag{15}$$

Hence combining yields

$$w \sim V_* + V_{*t} \tag{16}$$

or

$$L \sim (V_* + V_{*t})^2/g \tag{17}$$

where g is the acceleration due to the gravity of the planet. (The expressions for w and L are in good agreement with the numerically calculated values from the previous section.) Thus the material flux q is

$$q \sim \frac{\rho}{g}(V_* - V_{*t})(V_* + V_{*t})^2 \tag{18}$$

or

$$q = \frac{C}{g}\rho(V_* - V_{*t})(V_* + V_{*t})^2 \tag{19}$$

where C is the constant of proportionality.

On Mars there appear to be different interparticle forces as well as effects from changes in Reynolds number. These changes will alter the saltation characteristics by affecting the threshold friction speed. The flow field around individual particles (Knudsen and Reynolds numbers effects), shearing rate within the boundary layer, and the existence of comparatively large (to earth) viscous sublayer for nonsaltating flow will cause change in threshold values.

Low-Pressure Wind Tunnel Experiments

A series of wind tunnel tests was designed to explore the relation between eolian movement of surface material between terrestrial atmospheric pressures and low pressures equivalent of Mars. (A discussion of the wind tunnel test facility at NASA Ames Research Center is given by *Greeley et al.* [1977].) Using (18), a comparison between earth and Mars can be made:

$$\frac{q_E}{q_M} = \frac{\rho_E (V_* - V_{*t})_M g_M (V_* + V_{*t})_E^2 C_E}{\rho_M (V_* - V_{*t})_E g_E (V_* + V_{*t})_M^2 C_M} \tag{20}$$

where the C are constants of proportionality. Assuming that the ratio of friction speed to threshold friction speed, V_*/V_{*t}, is the same for both earth and Mars yields

$$\frac{q_E}{q_M} = \frac{\rho_E g_M (V_{*t})_E^3 C_E}{\rho_M g_E (V_{*t})_M^3 C_M} \tag{21}$$

Duplicating aerodynamic forces for typical conditions on Mars (temperature of 200 K and surface pressure of 0.75 kPa), the ambient pressure in the wind tunnel should be approximately 2.3 kPa. At this air pressure the gas density of the carbon dioxide on Mars is equal to the gas density of earth air in the wind tunnel. This creates equivalent dynamic pressures and, consequently, aerodynamic forces on the particles. Interparticle force equivalence should exist, since the ambient pressure is substantially reduced. The effects of gravity, not accounted in wind tunnel tests, can be adjusted to Mars.

The wind tunnel tests consist of spreading a uniform layer 1 cm thick of spherical glass bead particles (mean diameter of 0.208 mm) on the wind tunnel floor. At the end of the test section a material trap is placed. It consists of two uniform thin plates spaced 10 cm apart aligned parallel with the flow direction. The plates are from the floor to the ceiling of the wind tunnel. The front end (upstream side) is open to allow air flow to enter freely. The downstream end is sealed with #100 mesh wire to catch the particles yet still to allow a sizable amount of air to pass through so as not to alter greatly the flow field streamlines around the trap. The length of the trap is approximately 1 m long to prevernt rebounding particles off the back screen from bouncing out of the trap. The flow field is carefully observed, and no flow anomalies are found owing to the presence of the trap. The trap catches suspendable, saltating, and surface creeping particles. Knowing the width of the trap and the time of saltating, a material flux rate can be calculated.

First the terrestrial case is tested and found to be in agreement with theory. The test is repeated for a Martian surface condition of 0.75 kPa and temperature of 200 K. The results from both experiments are presented in Figure 8, which shows the mass flux q as a function of shear stress. At the lower pressure, substantially less stress is needed to move material. Furthermore, as the surface stress is increased, the lower pressure data show dramatic increases in mass flux, while the terrestrial data show only small increases in q. This notion supports the numerial results that show similar increases in particle path lengths. The path length is almost directly related to the mass flux. It would be useful if both cases could be adequately described by a single universal equation. According to the analytical derivation the only difference between the relations describing the two cases is the empirical constants C_E and C_M. If the constants of proportionality C_M and C_E are the same for both cases, this would indicate that the physics between the two tests remained unchanged. This implies a universality to the mass flux process. As one would expect, the process of movement of surface material on Mars should be nearly the same as the process on earth. Hence the constants of proportionality between the two test cases should be nearly the same. From the wind tunnel data of both pressure cases an empirical constant with a value of 2.61 was determined.

Figure 9 displays the mass flux versus a function of friction speeds. Here both high- and low-pressure data collapse to a single line in support of the idea of a universal function describing the movement process. Hence the following equation can be used in estimating mass flux on either earth or Mars once the friction speed and threshold friction speed are known:

$$q = 2.61 V_*^3 \rho (1 - V_{*t}/V_*)(1 + V_{*t}^2/V_*^2)/g \tag{22}$$

This must be considered the main contribution of the present work. The value of 2.61 is determined from the wind tunnel tests. A sensitivity study shows the constant to be stable over a range of altered conditions.

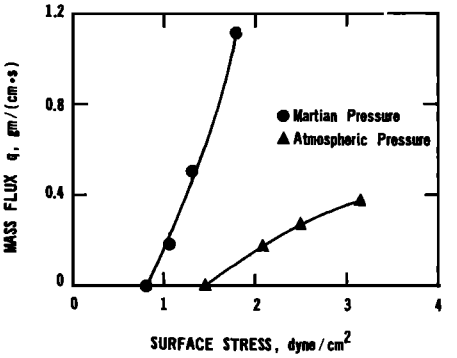

Fig. 8. Mass flux q as a function of the surface shear stress for wind tunnel tests. The circles are at 10^5 Pa, and the triangles are at 2.3 kPa. Tests were performed in the Marswitt wind tunnel located at NASA Ames Research Center.

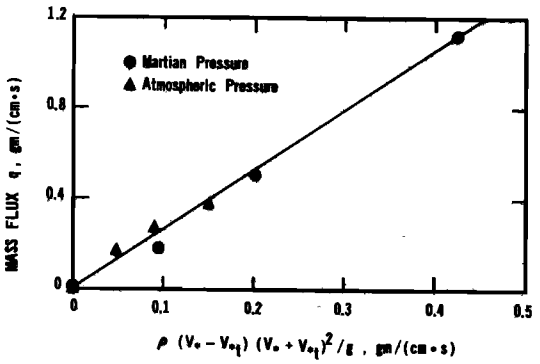

Fig. 9. Mass flux q as a function of the friction speed parameter. Here atmospheric and low-pressure data collapse to a single curve which is the straight line (equation (21)) on the plot. Note the origin data for both cases are data points, since they are used in determining the threshold friction speeds.

The flux of material on Mars is consistently higher than on earth. This increase is due to the existence of typically longer path lengths in the particle's trajectory and also to the reduction of gravity, which cannot be modeled in the wind tunnel. Moreover, using the established equation, the increase in q between the planets, assuming equal ratios of V_*/V_{*t}, is

$$q_M = \frac{(V_{*t}^3)_M}{(V_{*t}^3)_E} \frac{q_E}{13.5} \tag{23}$$

For instance, the relationship between the material movement on earth and on Mars, for equal ratios of V_*/V_{*t} of 1.47, would be $q_M/q_E = 6$, or 6 times as great on Mars for 0.2-mm particles.

Comparing the movement rates for similar dynamic conditions, equal ratios of B_*/V_{*t} on the two planets, yields

$$\frac{q_{\text{Mars}}}{q_{\text{earth}}} = 0.94 \frac{\rho_M g_E V_{*t_M}^3}{\rho_E g_{L_M} V_{*t_E}^3} \tag{24}$$

A direct estimate of flux rates on Mars can be made by employing the obtained result. The results are shown in Figure 10. To obtain a numerical value, the threshold friction speed must be known. The value will vary with size of particles, but once known, a direct estimate of the mass flux can be made. For example, assuming a 7.5-mbar (0.75 kPa) pressure at 200 K on the Martian surface for V_*/V_{*t} equal to 1.25, the flux rate q would be approximately 0.98 g/s cm. This is assuming V_{*t} equal to 1.75 m/s.

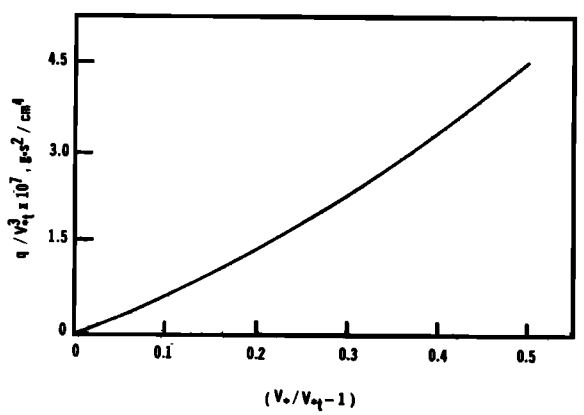

Fig. 10. The quantity q/V_{*t} as a function of the parameter $(V_*/V_{*t} - 1)$ for a typical Martian condition of 0.75 kPa, 200 K, and ρ_p from 2 to 3 g/cm³. Once V_{*t} is known, q can be determined from the curve.

SUMMARY AND CONCLUDING REMARKS

Numerical solutions of the equations of motion for particle trajectories on the surface of Mars are presented. The path lengths of saltating particles can vary as much as a factor of 2 where the minimum and maximum temperature recorded on the Martian surface by Viking 1 and 2 are considered. Typically, impacting particles collide at the surface with lower angles on Mars than on earth and have substantially more kinetic energy. Their kinetic energies can be up to 50 times greater on Mars than on earth for identical dynamic particle conditions. A discussion is presented on variations of these results with changing parameters. The ratio of final particle speed to the particle threshold friction speed is found to be several times larger than that of earth. For earth this ratio is known to be approximately one.

Wind tunnel tests performed at low-pressure and theoretical analysis are used to establish a transport equation of surface material on Mars. Wind tunnel data support the notion of a universal function to describe transport of surface material; e.g., both low- and high-pressure transport data are adequately described by a single transport equation. The transport equation can be used to estimate surface material flux on Mars with knowledge of both the threshold V_{*t} and V_*. Numerically integrated particle equations of motion provide information of mean path lengths and maximum heights of saltating particle trajectories on Mars for a range of conditions. Path lengths are from 3 to 10 m for 0.1- to 1-mm particles at wind speed slightly above threshold (0.75 kPa and 200 K). Consequently, saltating particles travel much faster and many times further on Mars in comparison to earth. Hence the transport equation shows many times the flux of surface material on Mars in comparison to dynamically similar conditions on earth. This result is verified by wind tunnel tests. Typically, under similar dynamic conditions, 5–10 times more surface material will be moved on Mars. This may seem misleading unless one considers that winds above particle threshold speeds do not occur nearly as often on Mars as compared to earth, as discovered by data received from the Viking spacecraft. However, when the Martian winds are above threshold, they are more efficient in moving surface material. This effect stems from two basic differences in the conditions. First, since the gravity on Mars is only 38% that of the earth, the particles do not return to the planets surface as rapidly. Second, the terminal particle speeds are substantially faster on Mars owing to the reduced pressure compared to earth. This creates longer path length on Mars, which directly increases the flux rate.

Acknowledgments. The author acknowledges Chi Tran for some of the calculations. The work is supported by the Office of Planetary Geology, National Aeronautics and Space Administration, through Interchange Agreement NCA 2-OR 180-605 to the University of California at Davis.

REFERENCES

Bagnold, R. A., *The Physics of Blown Sand and Desert Dunes*, pp. 39–76, Methuen, London, 1941.

Bird, R. B., W. E. Stewart, and E. N. Lightfoot, *Transport Phenomena*, pp. 21–24, John Wiley, New York, 1960.

Davies, C. N., Definitive equations for the fluid resistance of spheres, *Proc. Phys. Soc. London*, *4*(322), 259–270, 1945.

Greeley, R., B. R. White, J. B. Pollack, J. D. Iversen, and R. N. Leach, Dust storms of Mars: Considerations and simulations, *NASA Tech. Memo., TM 78423*, 1977.

Hess, S. L., R. M. Henry, C. B. Leovy, J. A. Ryan, J. E. Tillman, T. E. Chamberlain, H. L. Cole, R. G. Dutton, G. C. Greene, W. E. Simon and J. L. Mitchell, Mars climatology from Viking 1 after 20

sols, *Science, 195*(4260), 78–81, 1976.
Kawamura, R., Study of sand movement by wind (in Japanese), report, vol. 5, pp. 95–112, Tech. Res. Inst., Tokyo Univ., Tokyo, Japan, 1951.
Kliore, A. J., D. L. Cain, G. Fjeldbo, B. L. Seidel, M. E. Sykes, and S. I. Rasool, The atmosphere of Mars and from Mariner 9 radio occultation measurements, *Icarus, 17,* 484–516, 1972.
Kliore, A. J., G. Fjeldbo, B. L. Seidel, M. J. Sykes, and P. M. Woiceshyn, *S* band occultation measurements of the atmosphere and topography of Mars with Mariner 9: Extended mission coverage of polar and intermediate latitudes, *J. Geophys. Res., 78,* 4331–4351, 1973.
Morsi, S. A., and A. J. Alexander, An investigation of particle trajectories in two-phase flow systems, *J. Fluid Mech., 55*(2), 193–208, 1972.
Pollack, J. B., R. Haberle, R. Greeley, and J. D. Iversen, Estimates of the wind speeds required for particle motion on Mars, *Icarus, 29,* 395–417, 1976*a*.
Pollack, J. B., C. B. Leovy, Y. H. Mintz, and W. Van Camp, Winds on Mars during the Viking season: Predictions based on a general circulation model with topography, *Geophys. Res. Lett., 3*(8), 479–482, 1976*b*.
Sagan, C., and R. A. Bagnold, Fluid transport on earth and aeolian transport on Mars, *Icarus, 26,* 209–218, 1975.
Toon, O. B., J. B. Pollack, and C. Sagan, Physical properties of the particles composing the Martian dust storm of 1971–1972, *Icarus, 30,* 663–696, 1976.
Tsuchiya, Y., Mechanics of the successive saltation of a sand particle on a granular bed in a turbulent stream, *Disas. Prev. Res. Inst. Kyoto Univ. Bull., 19,* part 1(152), 31–44, 1969.
White, B. R., and J. C. Schulz, Magnus effect in saltation, *J. Fluid Mech., 81*(3), 497–512, 1977.
White, B. R., R. Greeley, J. D. Iversen, and J. B. Pollack, Estimated grain saltation in a Martian atmosphere, *J. Geophys. Res., 81,* 5643–5650, 1976.
Yaalon, D. H., and E. Ganor, Origin and nature of desert dust, in *Proceedings of the Desert Dust Symposium,* edited by T. J. Péwé, American Association for the Advancement of Science, Washington, D. C., 1977.

(Received October 17, 1977;
revised September 24, 1978;
accepted February 1, 1979.)